Supporting Information

Transformation Study and Characterization of Cu-BTC MOF-derived Nanoporous Copper Oxide

Sameh Khalil, Abhijit Ganguly, Davide Mariotti, and Supriya Chakrabarti*

School of Engineering, Ulster University, York St, Belfast BT15 1AP, UK

*Corresponding Author: s.chakrabarti@ulster.ac.uk

S1. Crystalline structure of Cu-BTC

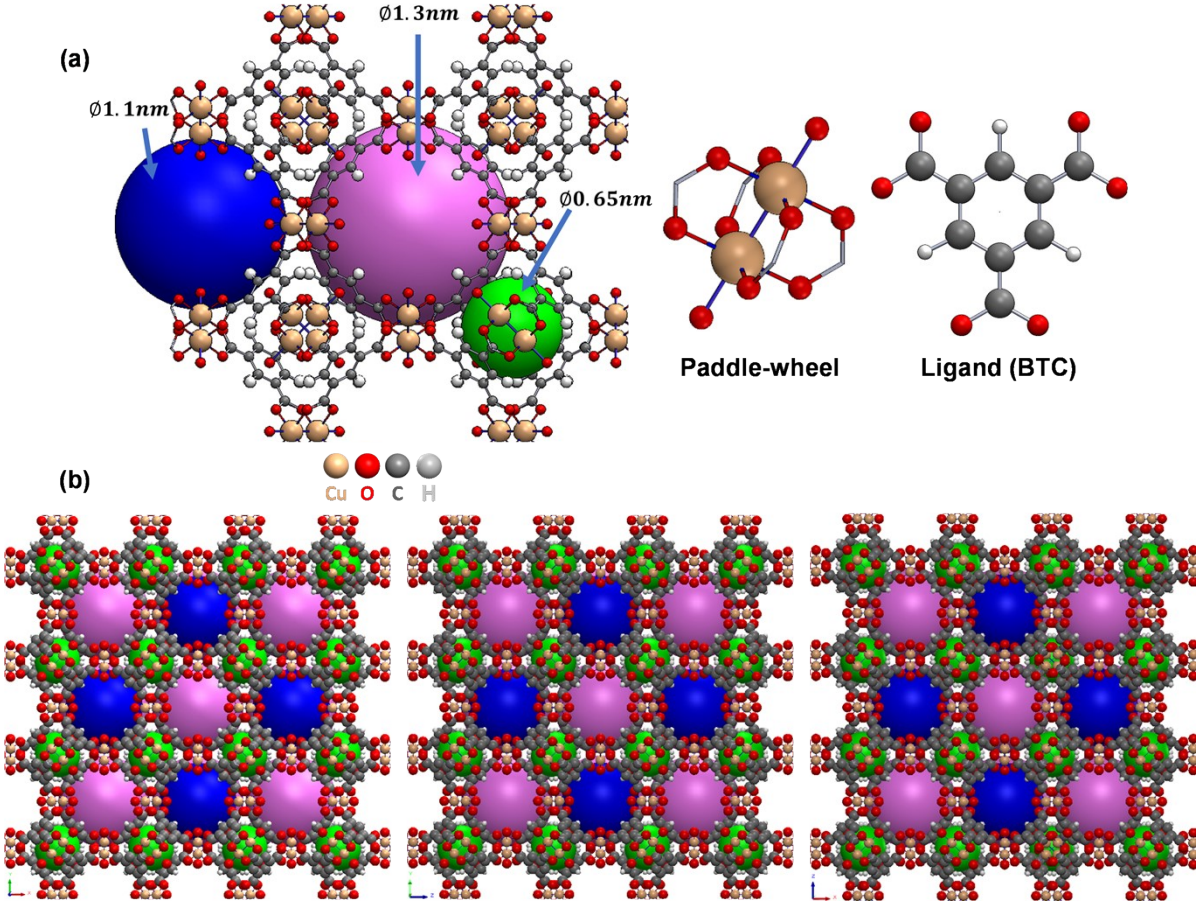

Fig. S1. The crystalline structure of Cu-BTC MOF; a) The unit cell with three pore sizes, b) 3D views for 8-unit cells of Cu-BTC including the pores, showing how the structure extends in 3D. The pores sizes are matches with the literature.[1] The atomic coordinates of the framework atoms were taken from the literature.[2,3]

S2. Additional figures for characterization

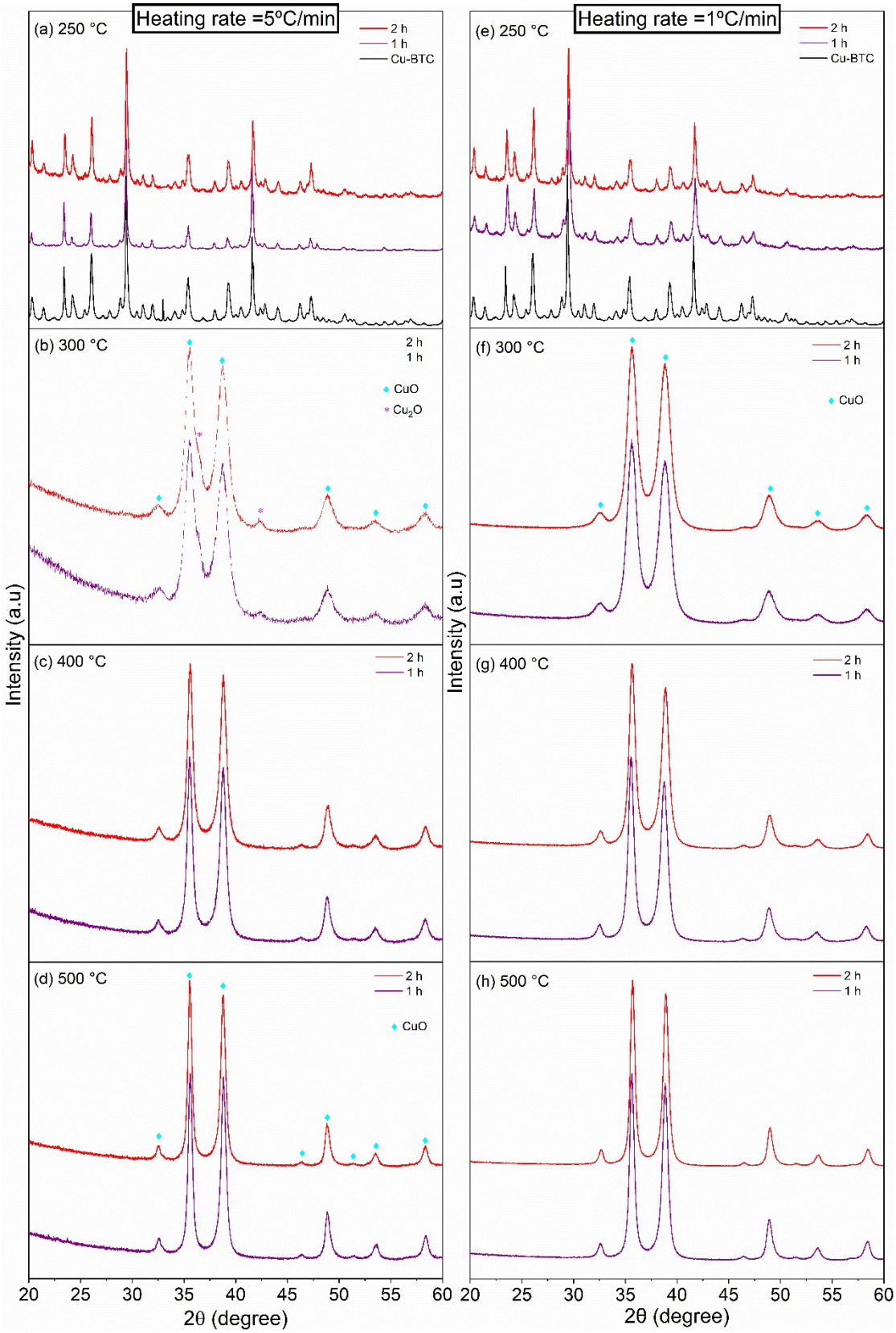

Fig. S2. XRD patterns of Cu-BTC-derived samples synthesized at different calcination temperatures (T_C), a&e) 250°C, b&f) 300°C, c&g) 400°C, and d&h) 500°C, with the heating rate (HR) of 5°C/min (left column) and 1°C/min (right column).

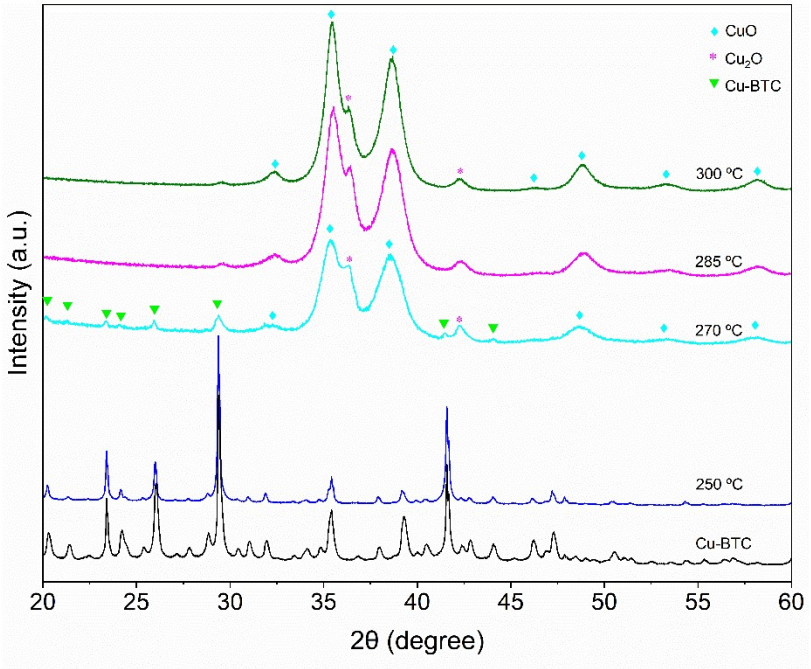

Fig. S3. XRD patterns of Cu-BTC-derived samples synthesized at different calcination temperatures (T_C), with the heating rate (HR) of 5°C/min for 1h duration.

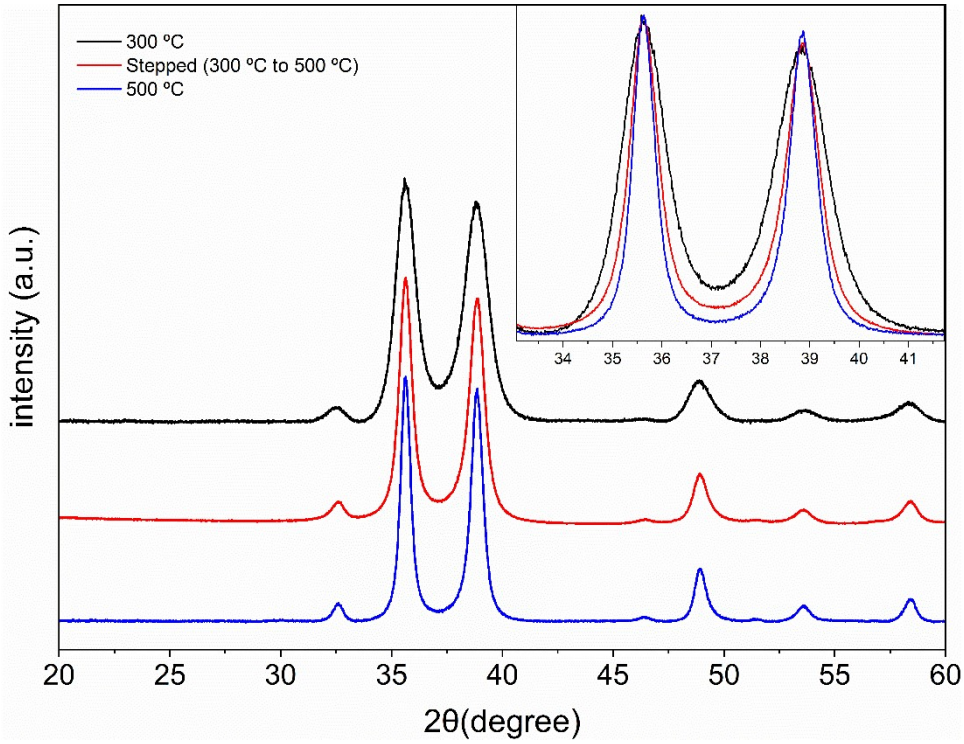

Fig. S4. XRD patterns of P-CuO synthesized under different conditions: direct calcination at 300 and 500°C (HR of 1°C/min & for 1h), stepwise calcination where the sample was first calcined at 300°C (HR of 1°C/min for 1h) followed by an additional 1h calcination at 500°C.

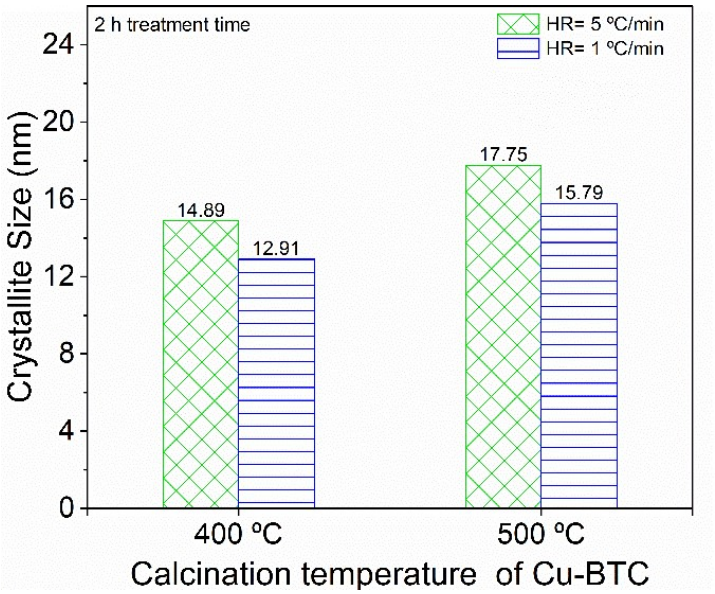

Fig. S5. Crystallite size (estimated from XRD data) of the synthesized P-CuO_x samples at T_C of 400 and 500°C for 2h, comparing different HR (5°C/min and 1°C/min).

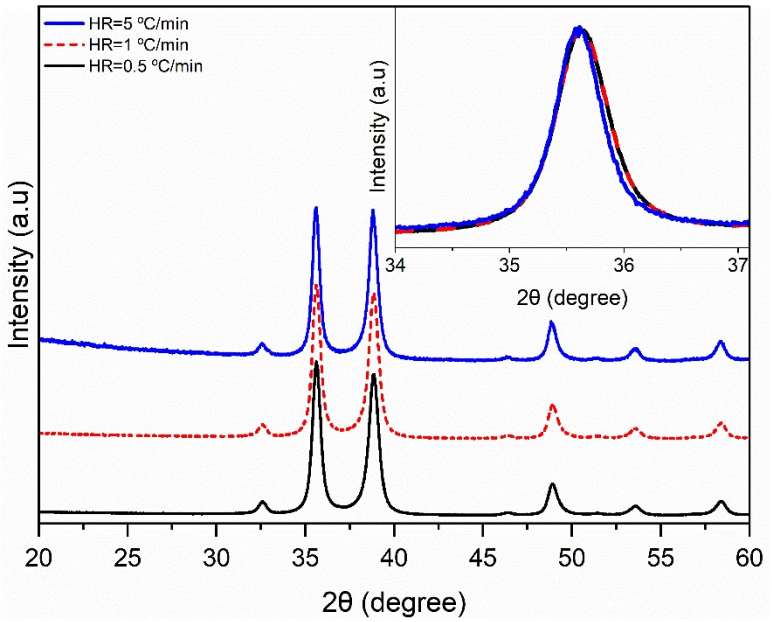

Fig. S6. XRD patterns of P-CuO synthesized at T_C of 500°C with different heating rates.

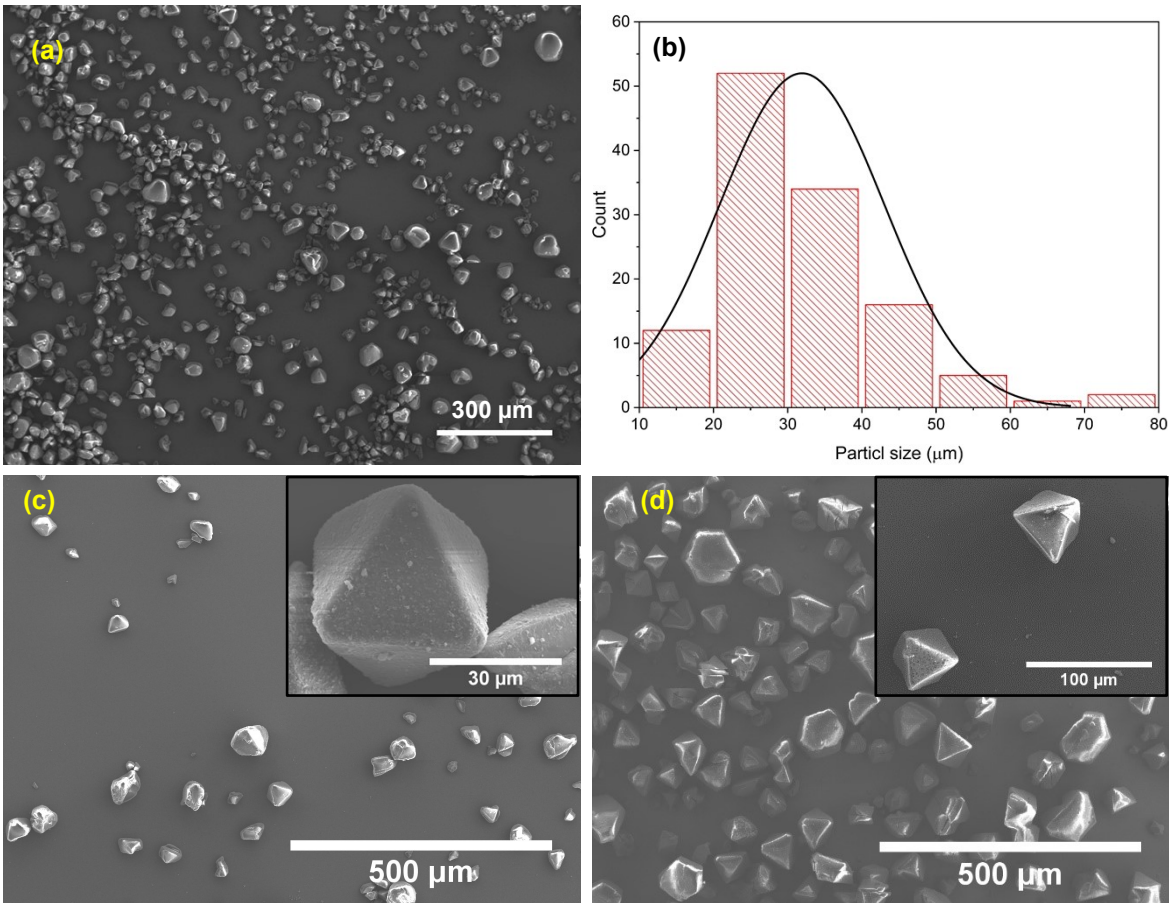

Fig. S7. a&b) Typical SEM image (a) and corresponding histogram (b) representing the particle size distribution of pristine Cu-BTC MOF. c&d) SEM images of (c) pristine Cu-BTC and (d) the sample calcinated at T_C of 250°C (with HR of 5°C/min for 1h).

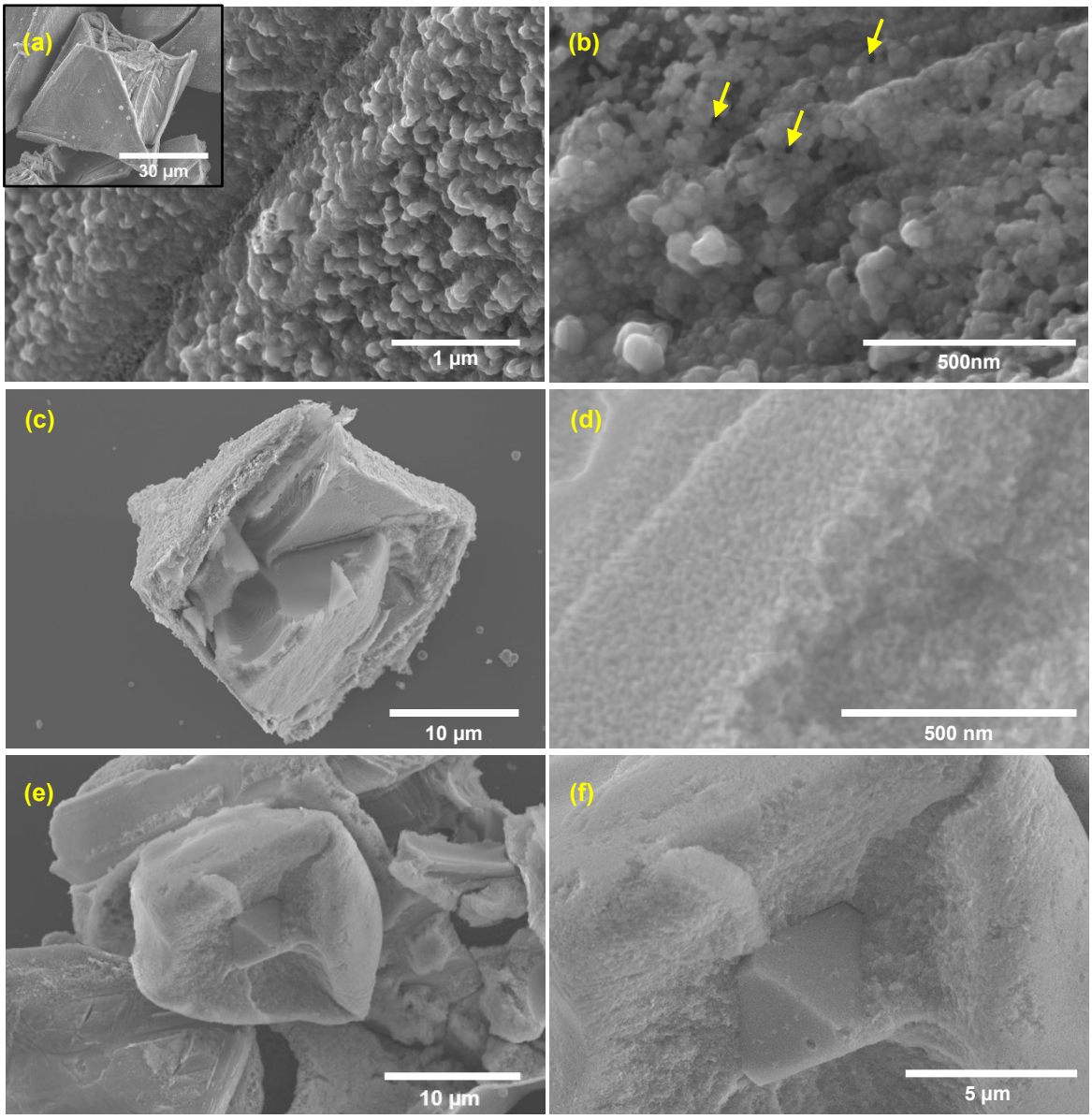

Fig. S8. Magnified SEM images presenting the internal morphology of the synthesised P-CuO (T_C of 500°C, with HR of 5°C/min for 1h).

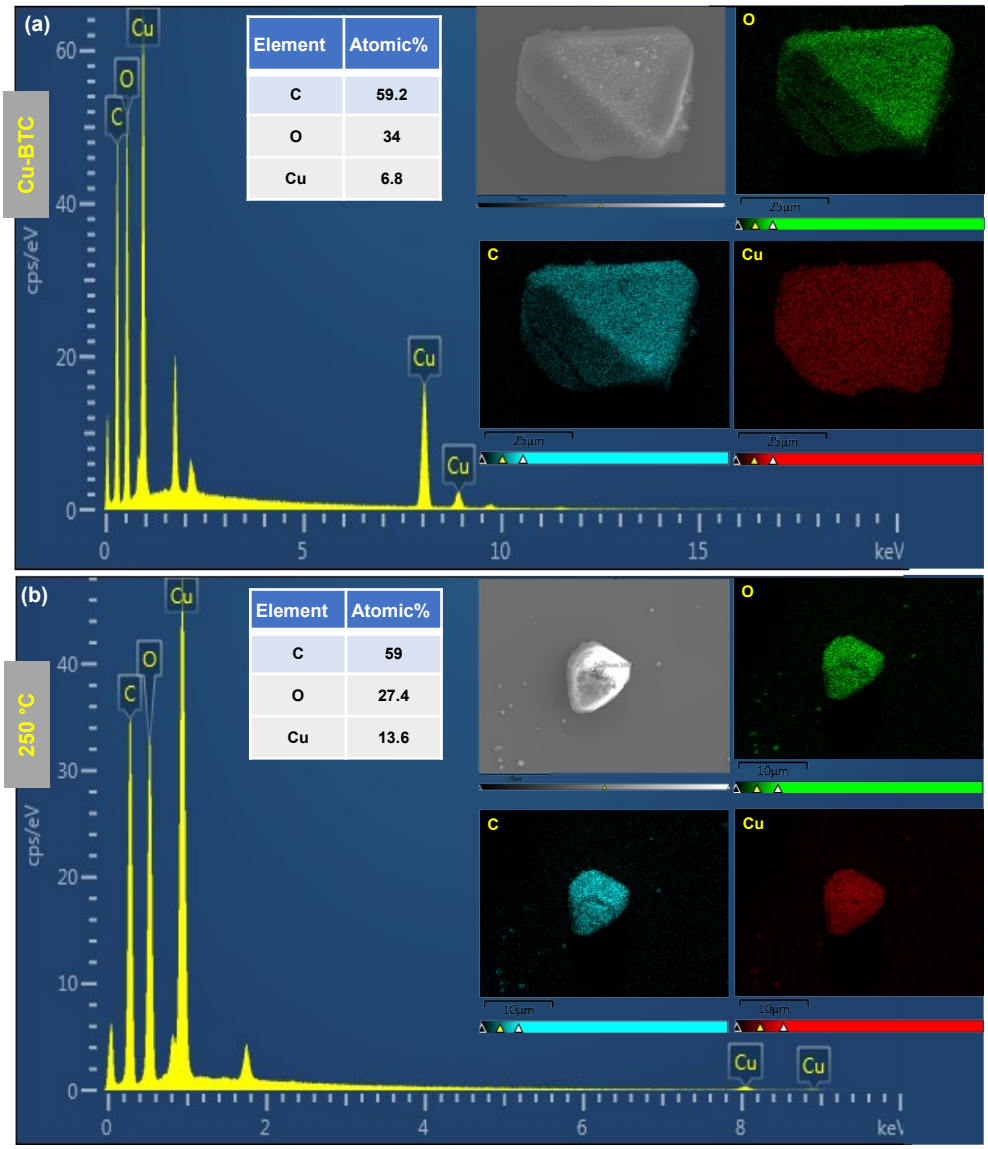

Fig. S9. EDX spectra with elemental mapping of a) pristine Cu-BTC, and b) the sample calcinated at T_C of 250°C (HR of 5°C/min for 1h). The insets present the SEM images for the corresponding samples as well as the elemental distribution of C, O, and Cu.

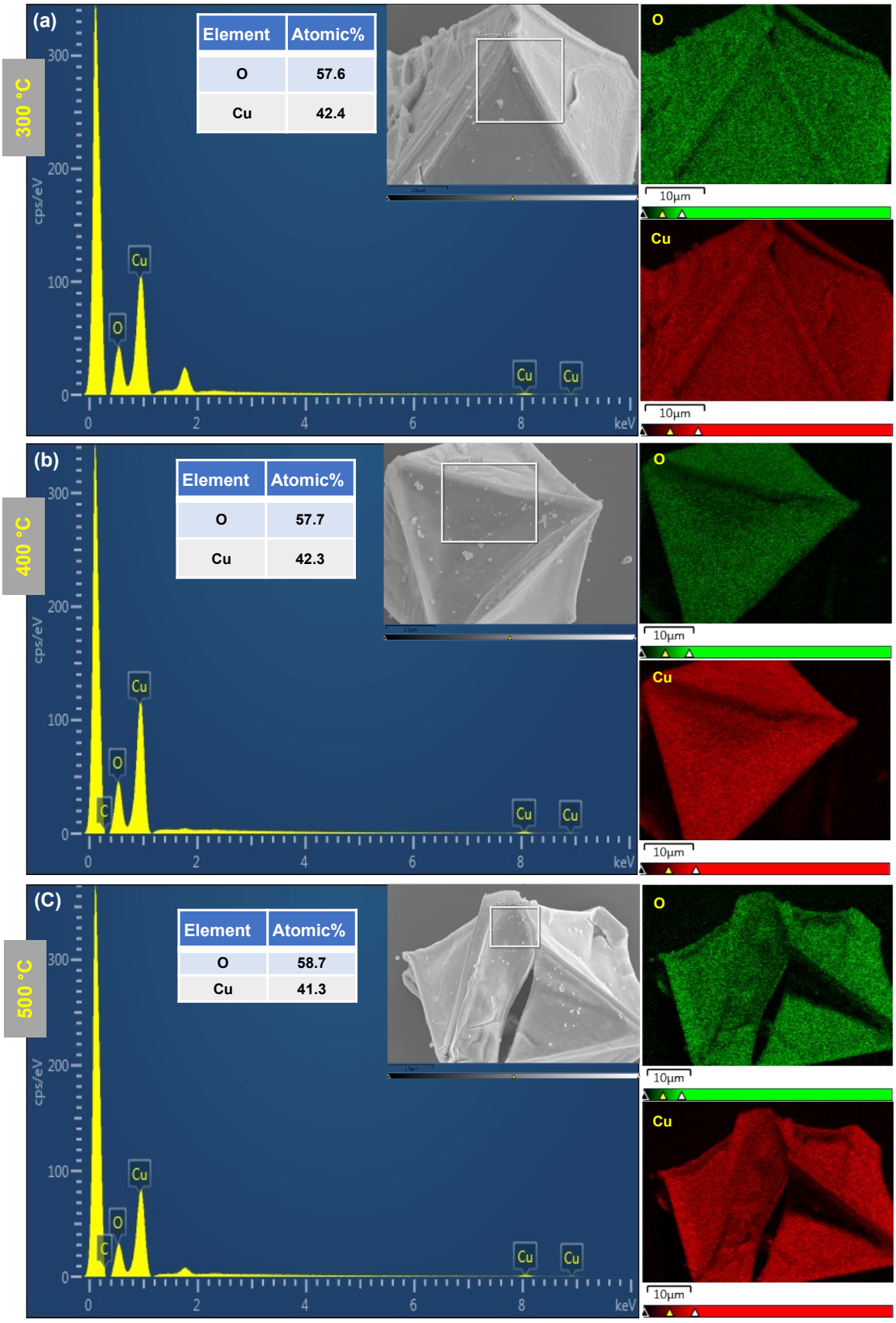

Fig. S10. EDX spectra with elemental mapping of the synthesized P-CuO_x samples at different T_C, a) 300°C, b) 400°C, and c) 500°C (HR of 5°C/min for 1h). The insets present the SEM images for the corresponding samples as well as the elemental distribution of O, and Cu.

S3. Raman Analysis

For further analysis of the chemical structure and molecular vibration modes of the samples, Raman spectroscopy was employed on the samples which were calcinated with HR of 5°C/min. Raman spectra for all samples were recorded as presented in Fig. S11. Samples calcinated at 250°C showed Raman shifts associated with Cu-BTC. The Raman spectra indicated that all Raman shifts were in consistent with those recorded in literatures.[4] Upon calcination at 300°C, Raman peaks presented the existence of both Cu_2O and CuO phases. The peaks observed at 110, 146, 217, 415, and 525 cm^{-1} were attributed to Cu_2O [5,6], while the peaks at 292, 340, 627, and 1130 cm^{-1} were associated with CuO.[7–9] Notably, the Cu_2O peak at 110 cm−1 is related to the inactive Raman mode. The peaks at 146, 217, 415, and 525 cm^{-1} correspond to the second-order overtones Γ_{15} $^{(1)}$, $2\Gamma_{12}$, $2\Gamma_{15}$ $^{(1)}$, and $2\Gamma_{15}$ $^{(1)}$ respectively.[6,10] By increasing the temperature T_C to 400 and 500 °C, Raman spectra indicated peaks related to single phase CuO. CuO typically exhibits three active Raman modes, denoted as (A_g+2B_g).[9] Upon examination of the vibrational spectra, the peak located at 292 was assigned to the A_g mode, while, peaks at 340 and 627 cm^{-1} were attributed to the B_g mode.[9] Additionally, the peak at 1130 cm^{-1} was identified as a multi-phonon band 2B_g.[11]

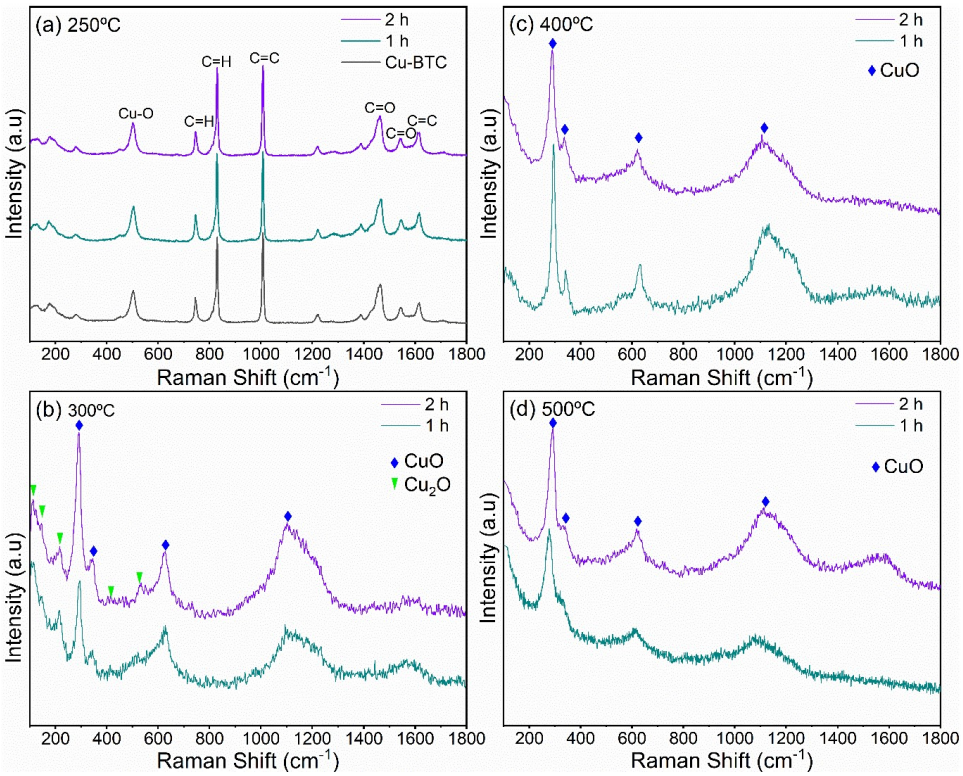

Fig. S11. Raman spectra of the synthesized P-CuO_x samples at different T_C, a) 250°C, b) 300°C, c) 400°C, and d) 500°C, with HR of 5°C/min.

S4. XPS survey spectra

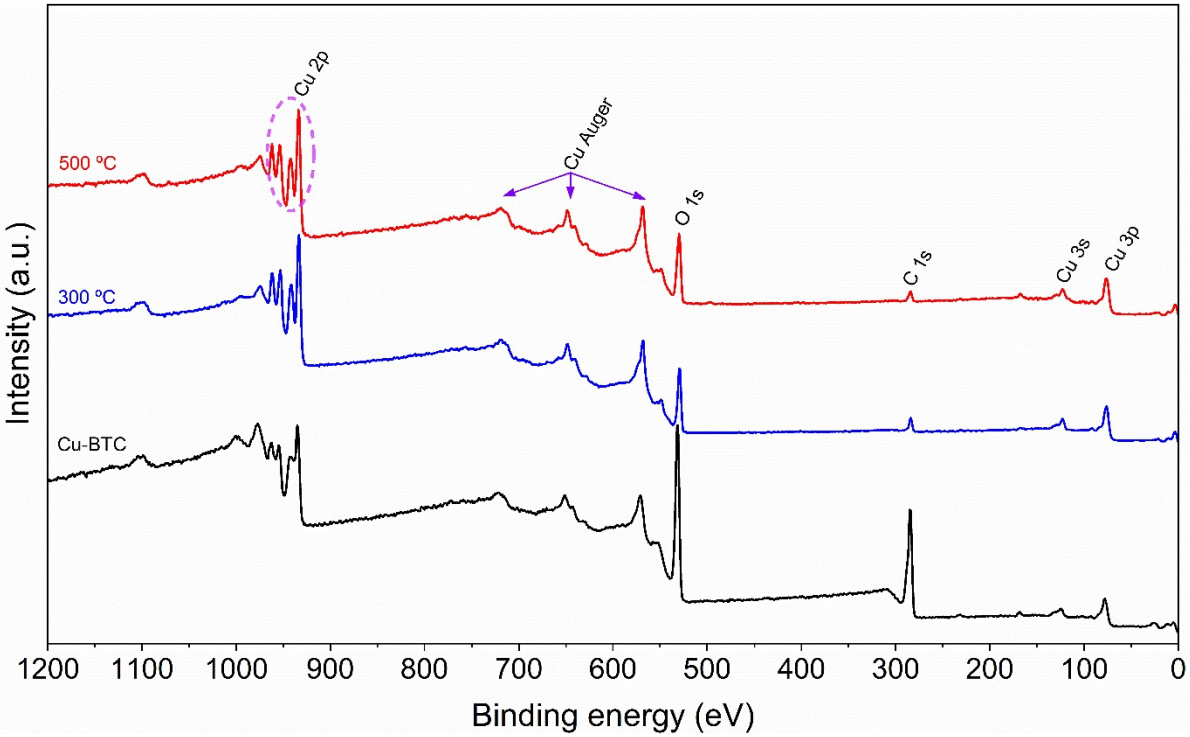

Fig. S12. XPS survey spectrua of pristine Cu-BTC, and the synthesized P-CuO_x samples at T_C of 300 and 500°C (HR of 5°C/min for 1h).

Table S1. Surface elemental composition (At. %) measured from XPS analysis for pristine Cu-BTC, and the synthesized P-CuO_x samples at T_C of 300 and 500°C (HR of 5°C/min for 1h).

Sample	Elements		
	C	O	Cu
Cu-BTC	51.05	39.65	9.30
300°C	16.88	37.75	45.37
500°C	15.98	41.2	42.82

Table S2. Peak fitting results of O 1s XPS spectra obtained for pristine Cu-BTC, and the synthesized P-CuO_x samples at T_C of 300 and 500°C (HR of 5°C/min for 1h).

Sample	Component	Binding Energy (eV)	FWHM (eV)	At. %
Cu-BTC	Cu-O-C	532.75	2.05	100
300°C	O=Cu	529.03	1.02	39.06
	O-H	530.77	1.71	33.06
	O-C	532.62	1.85	27.88
500°C	O=Cu	529.01	1.04	46.78
	O-H	530.78	1.87	32.95
	O-C	532.5	1.86	20.27

S5. Determination of the Work function

Ultraviolet photoelectron spectroscopy (UPS) spectra, Fig. S13, showed the cut-off ($E_{Cut\text{-}off}$) and the on-set ($E_{On\text{-}set}$) energies for Cu-BTC and the calcinated sample at 500°C. The UPS spectrum's on-set energy, which is known as the valence band edge, is the lowest energy at which electrons start to emit from the sample surface. This represents the energy of the highest-energy electrons in the valence band of the material, which are just able to escape the surface and be detected by the analyzer. In contrast, the cut-off in the UPS spectrum is the highest energy at which electrons can be detected. It is determined by the energy of the incident UV photons and the work function (φ) of the material. Electrons with energies above the cut-off cannot escape from the material surface and therefore cannot be detected by the analyzer. The work function of a material is the energy difference between its Fermi energy (E_F) and the vacuum energy level (E_{Vac}) and could be calculated as; $\varphi = h\nu - (E_{Cut\text{-}off} - E_F)$ [12], where $h\nu$ is energy of the incident photon which is 21.22 eV. From the UPS spectra, the on-set and cut-off energies for Cu-BTC were found to be 1.85 eV and 19.03 eV, respectively, while for P-CuO at 500 °C, they were 0.56 eV and 17.5 eV. Using the onset and cut-off energies, the work function was determined to be 2.19 eV for Cu-BTC, and 3.72 eV for P-CuO.

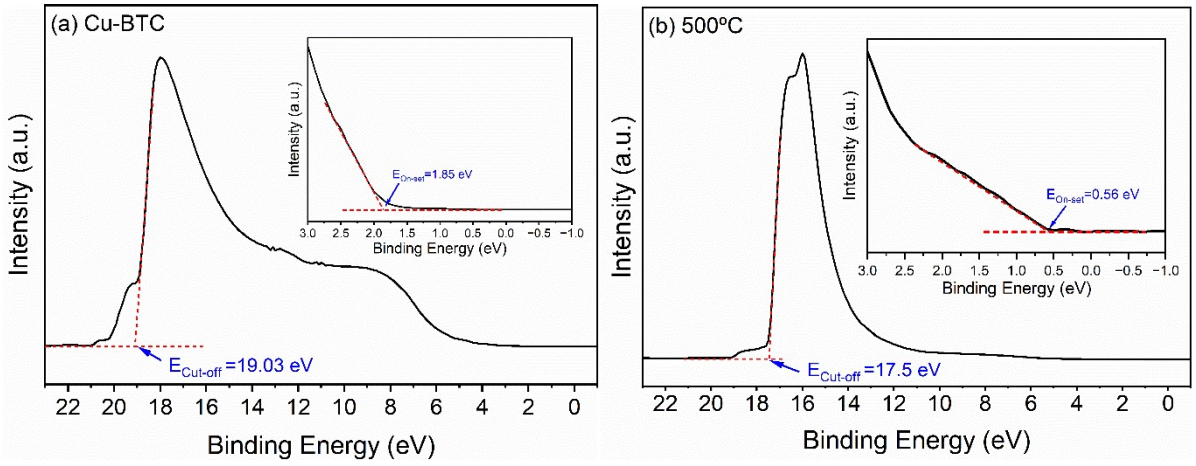

Fig. S13. UPS spectra of (a) pristine Cu-BTC and (b) P-CuO_x sample calcinated at T_C of 500°C (HR of 5°C/min for 1h).

S6. Adsorption–desorption isotherms of Cu-BTC

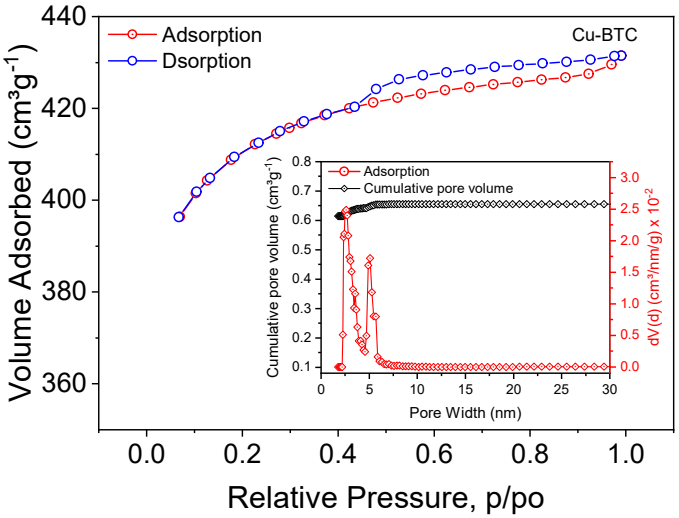

Fig. S14. N_2 Adsorption–desorption isotherms, with inset detailing the pore-volume and pore width for pristine Cu-BTC MOF.

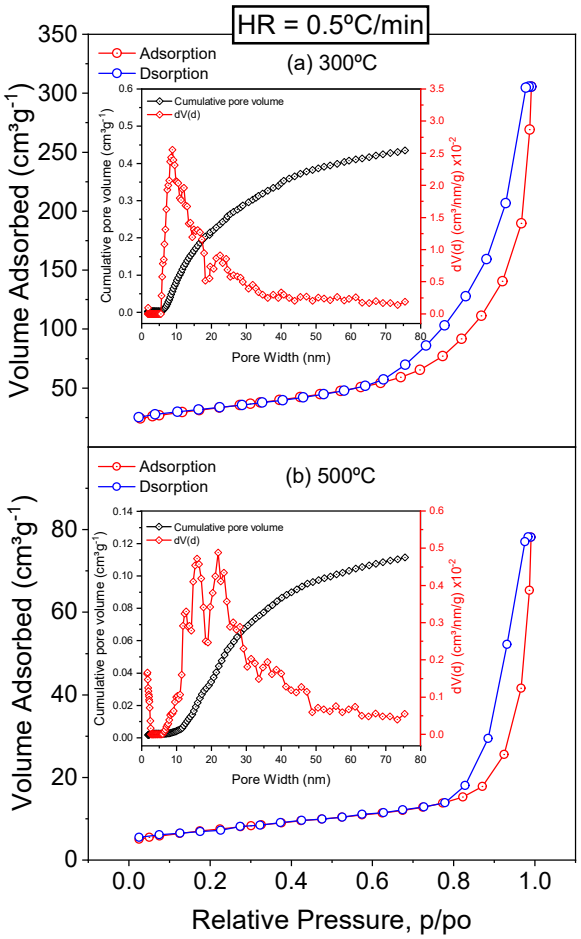

Fig. S15. N_2 Adsorption–desorption isotherms, with insets presenting the corresponding pore size distribution, for the synthesized P-CuO_x at T_C of 300°C (a), and 500°C (b), with HR of 0.5°C/min, for 1h duration.

S7. Tauc plot for band gap

From the absorption coefficient, Tauc plot could be generated for band gap calculation. For semiconductor, band gap could be determined according to relation $(\alpha h\nu)^n = k\,(h\nu - E_g)$ [13], where α is the absorption coefficient, h is Planck's constant, ν is the frequency of the absorbed light, K is a constant, and E_g is the optical band gap energy. The value of n could be 2 or ½ for direct and indirect electron transition respectively. The plot was created by plotting a function of the absorption coefficient as a function of photon energy. The graph generated by plotting $(\alpha h\nu)^2$ against $(h\nu)$ for a direct band gap, and the value of E_g could be determined by obtaining the tangent to the graph and identify the point where it intercepts the abscissa, as shown in Fig. S16.

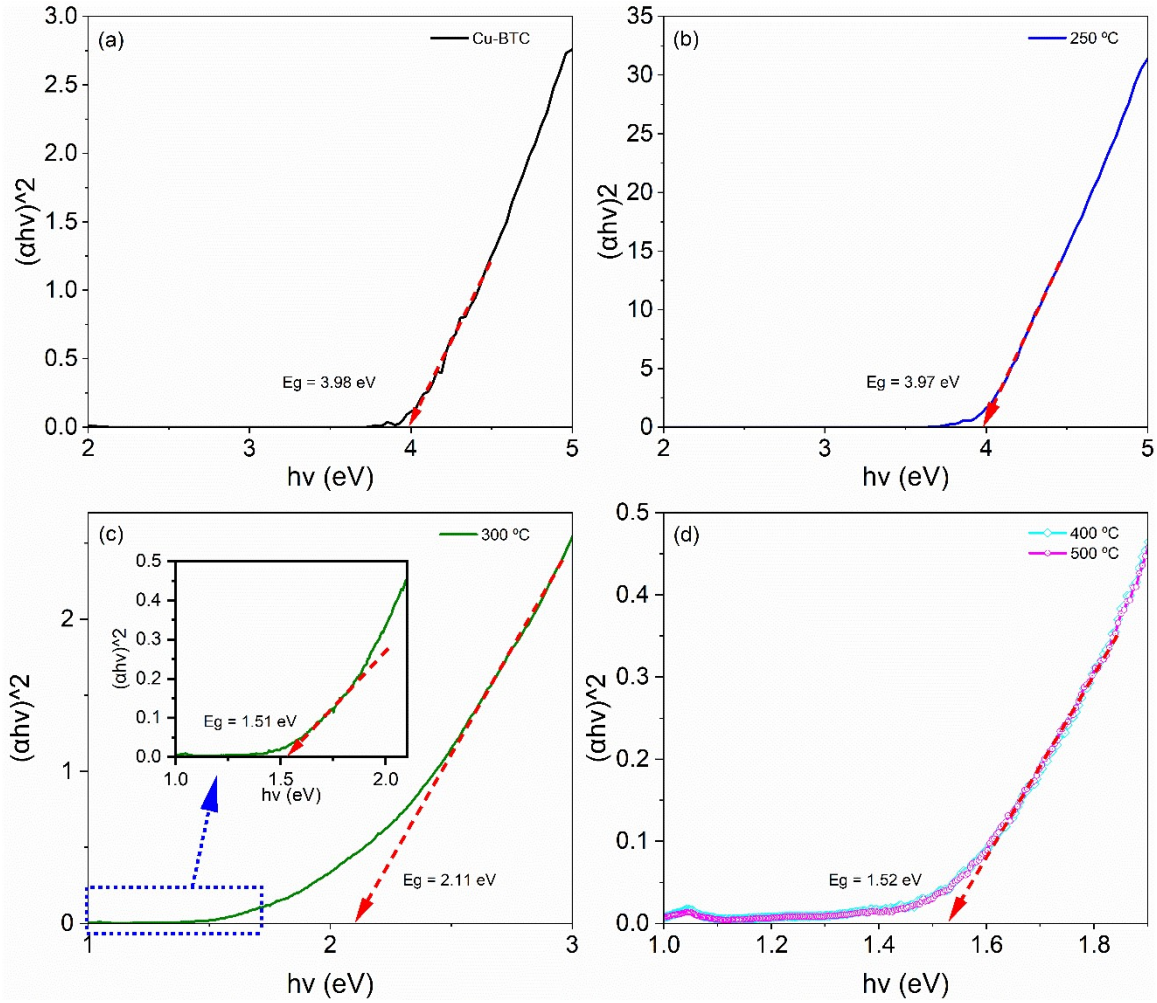

Fig. S16. Band gap estimation from Tauc plot for a) pristine Cu-BTC, and b-d) The synthesized P-CuO_x samples at different T_C, b) 250°C, c) 300°C, and d) 400°C and 500°C (HR of 5°C/min for 1h).

Table S3: Band gap values, estimated from Tauc plot and REELS analysis, of pristine Cu-BTC, and the synthesized P-CuOx samples at different T_C (HR of 5°C/min for 1h).

Technique	Band gap (E_g)				
	Cu-BTC	**250 °C**	**300 °C**	**400 °C**	**500 °C**
Tauc plot	3.98	3.97	1.51 & 2.11	1.52	1.52
REELS	3.36		1.45 & 2.07	1.44	1.41

References

1 V. Zeleňák, I. Saldan, *Nanomaterials* **2021**, *11*, 1638.

2 W. Wong-Ng, J. A. Kaduk, D. L. Siderius, A. L. Allen, L. Espinal, B. M. Boyerinas, I. Levin, M. R. Suchomel, J. Ilavsky, L. Li, *Powder Diffr.* **2015**, *30*, 2–13.

3 S. S.-Y. Chui, S. M.-F. Lo, J. P. H. Charmant, A. G. Orpen, I. D. Williams, *Science (80-.).* **1999**, *283*, 1148–1150.

4 Y. Wang, W. Cao, L. Wang, Q. Zhuang, Y. Ni, *Microchim. Acta* **2018**, *185*, 1–9.

5 J. He, Y. Jiang, J. Peng, C. Li, B. Yan, X. Wang, *J. Mater. Sci.* **2016**, *51*, 9696–9704.

6 P. K. Pagare, A. P. Torane, *Microchim. Acta* **2016**, *183*, 2983–2989.

7 J. F. Xu, W. Ji, Z. X. Shen, W. S. Li, S. H. Tang, X. R. Ye, D. Z. Jia, X. Q. Xin, *J. Raman Spectrosc.* **1999**, *30*, 413–415.

8 S. Choudhary, J. V. N. Sarma, S. Pande, S. Ababou-Girard, P. Turban, B. Lepine, S. Gangopadhyay, *AIP Adv.* **2018**, *8*.

9 O. Prakash, S. Kumar, P. Singh, V. Deckert, S. Chatterjee, A. K. Ghosh, R. K. Singh, *J. Raman Spectrosc.* **2016**, *47*, 813–818.

10 M. C. Huang, T. Wang, W. S. Chang, J. C. Lin, C. C. Wu, I. C. Chen, K. C. Peng, S. W. Lee, *Appl. Surf. Sci.* **2014**, *301*, 369–377.

11 W. Wang, Q. Zhou, X. Fei, Y. He, P. Zhang, G. Zhang, L. Peng, W. Xie, *CrystEngComm* **2010**, *12*, 2232–2237.

12 J. W. Kim, A. Kim, H. U. Hwang, J. H. Kim, S. Choi, N. Koch, D. Shin, Z. Zhao, F. Liu, M. Choi, *J. Vac. Sci. Technol. A* **2023**, *41*.

13 Y. Yang, D. Xu, Q. Wu, P. Diao, *Sci. Rep.* **2016**, *6*, 1–13.